T031502_AD8151.pdf

Heavy-Ion Testing of the AD8151 Cross-Point Switch

Texas A&M University Cyclotron Institute

15th March, 2002

S. Buchner, J. Howard, and M. Carts
NASA/GSFC
Code 561.4
Greenbelt MD 20771

1. Introduction

Single Event Effects testing of the AD8151, a fabric-based switch, was carried out using heavy ions at Texas A&M University's Cyclotron Institute. A single part was tested due to the difficulty of changing parts soldered to the evaluation board. SEEs were measured as a function of number of paths through the switch, the data rate and ion LET.

2. Device Description

The AD8151 Crosspoint switch manufactured by Analog Devices is designed to connect any (or all) of 33 inputs to any (or all) of 17 outputs with a maximum throughput of 3.2 Gbps. Because of its low power and high speed, it has potential applications in space for optical network switching or for a Giga-bit ethernet.

Fig. 1 shows the functional block diagram of the AD8151. Inputs are connected to outputs by connecting or disconnecting the appropriate switches in a two dimensional array. The state of each switch, whether "on" or "off", is controlled by configuration data stored in a latch. The data are loaded into the latch through a series of programming steps. The first step is to load all the configuration data sequentially into a "first rank" latch. The data are then strobed simultaneously into a "second-rank" latch. The outputs of the second rank latch are decoded and drive the individual switches in the 33 by 17 matrix.

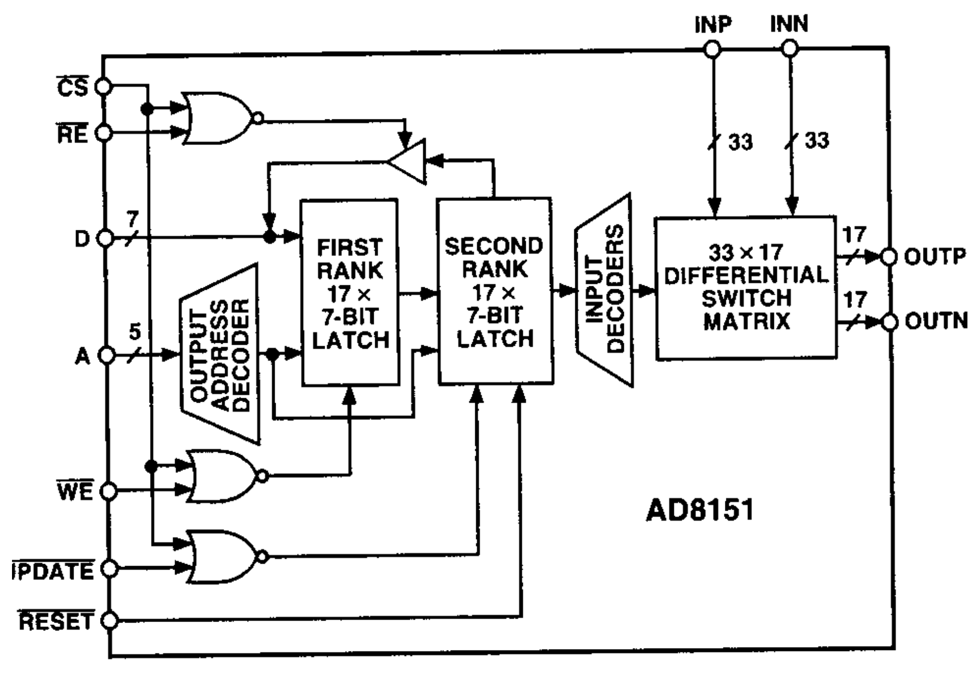

Figure 1. Functional Block diagram of the AD8151 showing the first and second rank latches as well as the switch matrix connecting any input to any output.

The latches are manufactured in CMOS technology and the switches in bipolar technology. Figure 2 shows the bipolar components used in the switch. Ion strikes in the latch will cause a SEU that may disrupt communications and manifest itself as a loss of synchronization (LOS). An ion strike in the decoder or the switch itself could cause a temporary change in the state of the switch, interrupting data transmission for a short time. These types of SEUs could cause single bit errors or bursts of errors, depending on how long it takes the switch to recover.

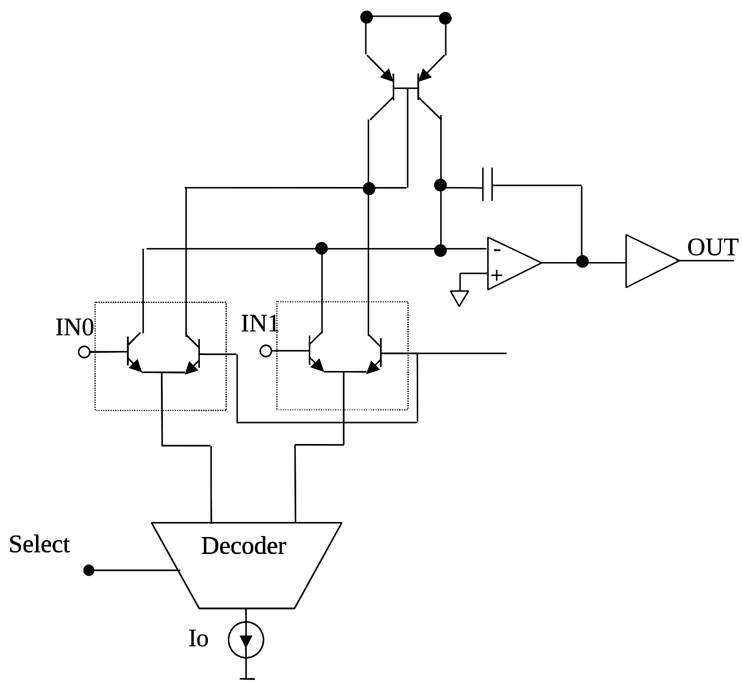

Figure 2. Circuit components used for constructing a switch.

For testing, the manufacturer provided a part mounted on an evaluation board together with software for programming the switch. However, for programmatic control, Labview drivers were developed and used instead. Two lines are required for all input and output ports because the part is a fully differential non-blocking array. The device is packaged in a plastic 184 lead LQFP (leaded quad flat pack) with 16 mil lead pitch. Prior to testing, the plastic over the die was removed by first grinding a depression in the plastic and then filling the depression with acid. Figure 3 shows the die and the bond wires leading into the plastic encapsulant.

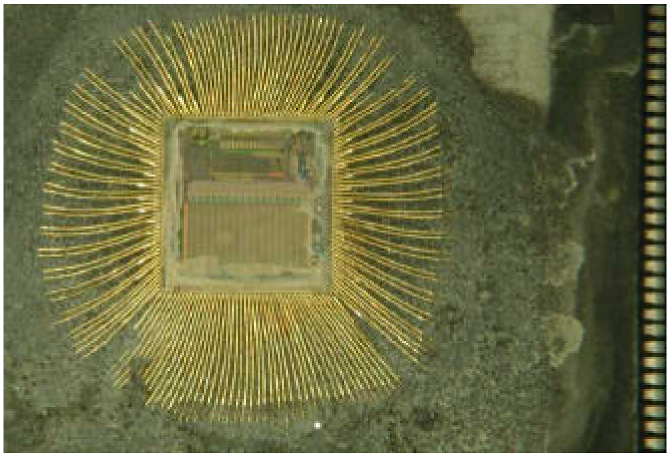

Figure 3. Closeup picture of the AD8151 die and bond wires.

3. Test Setup

A bit error-rate tester (BERT) was used for SEE testing of the switch. The BERT supplied a serial data stream to a switch input. After passing through the switch, the output was fed back to the BERT and compared with the original data pattern. Any differences were flagged as SETs. The signals supplied by the BERT to the switch were a standard, pseudo-random 127 bit repeating sequence pattern having a peak-to-peak differential from –0.75 V to + 1.5 V. The data rate was varied for different runs. High performance (18 GHz) cables were used for all RF signals.

The switch was programmed using the software drivers written in Labview and incorporated into the test application. Two different matrix configurations were used. In the first the data stream made one pass through the matrix. In the second the data stream passed through the switch five times. This was achieved by connecting four outputs to four inputs and defining the matrix configuration in such a way as to have a continuous path through the AD8151. The rational for this approach was to ascertain whether the BER or the LOS cross-section depended on the switch configuration. Figure 2 shows the switch configurations for both cases. The path is as follows:

BERTout➔**I**10→**O**0➔**I**13→**O**2➔**I**8→**O**6➔**I**28→**O**16➔**I**18→**O**10➔BERTin,

where the bold arrows (➔) are external coaxial cables and the regular arrows (→) are internal paths thru the AD8151. In the single path case the switch configuration is:

BERTout➔**I**10→**O**0➔BERT(in)

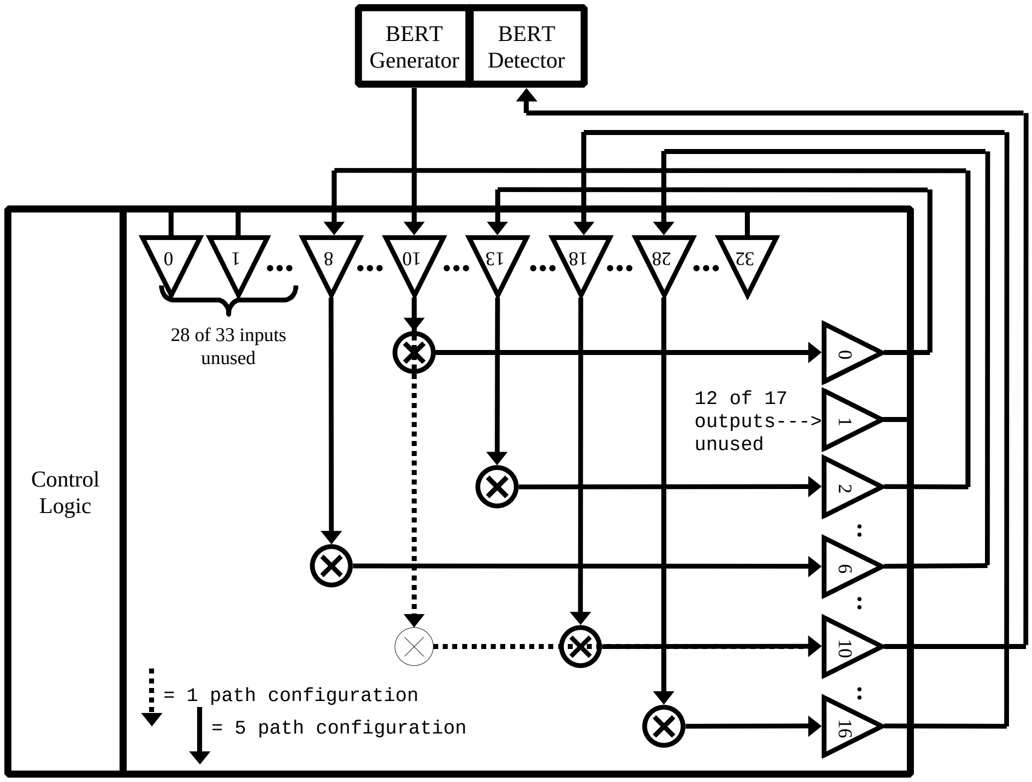

Figure 4. Diagram of the internal and external connections for the 5-path and 1-path configurations for the AD8151 crossbar switch.

4. SEE Test Results

Table 1 lists all the pertinent details for each exposure. The standard information, such as ion species, ion LET, angle of incidence, flux, exposure time and fluence are included. Only one device (device #3) was tested with I_V_{ee} = 3.2 V. The table also contains information regarding operation of the device, such as data rate and number of paths through the device. In addition, the table lists the three types of errors encountered during the measurements. The first type is single bit errors characterized by a single bit flip in the data stream. There is no long-term disruption to data transmission associated with a single bit error. The second type consists of a burst of errors, which is a continuous series of errors of finite length. Once the burst is over, transmission of correct data resumes. The third type of error is a LOS by the BERT due to a loss of the transmitted signal as a result of a SEU in the latch that changes the configuration. A LOS requires that the configuration data be reloaded into the AD8151 latch. In most cases at least two runs were made for each set of experimental conditions and the average was computed.

The exposure time is a critical parameter because it is needed to measure the BER. During the experiment, transmission was started before the beam was turned on and the beam was stopped as quickly as possible following a LOS or after a predetermined fluence. The bit error-rate is determined by dividing the number of errors by the number of bits transmitted, where the number of transmitted bits is obtained by multiplying the data rate by the exposure time. Therefore, the BER is given by:

$$BER = \frac{\#errors}{(time) \bullet (data\_rate)}$$

The BER was calculated for both single-bit errors and burst errors as a function of ion LET, data rate and number of paths through the switch. The average length of a burst of errors was calculated by taking the ratio of the total number of bit errors in bursts to the total number of bursts. That value was plotted as a function of ion LET for different data rates and number of paths through the switch.

Figure 5 shows the BER for single bit errors for five paths through the switch for different data rates as a function of ion LET. The single BER has a threshold below 2.86 MeV.cm^2/mg. The single BER initially increases with LET and then shows a sharp decrease above a LET of about 9 MeV.cm^2/mg. Above an LET of 12 MeV.cm2/mg the single BER increases again. There BER also depends on data rate, but the explanation is not obvious.

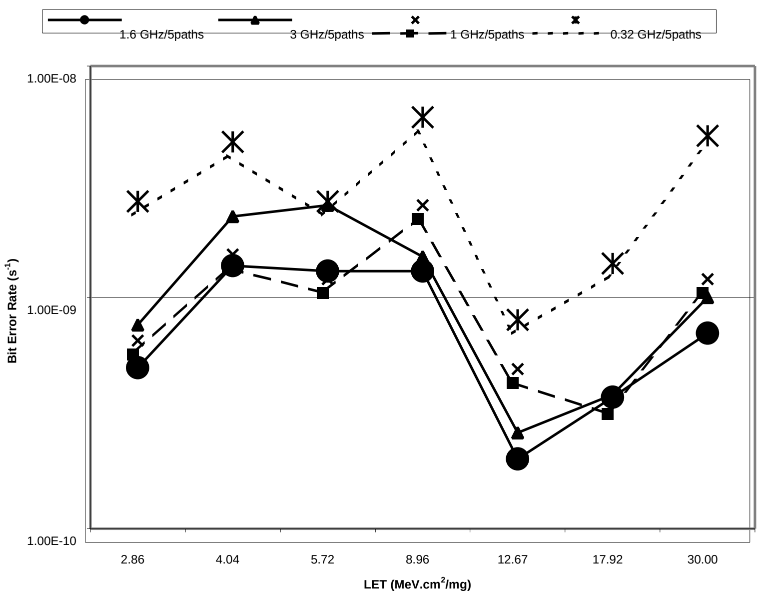

Figure 5. Single-bit error rate as a function of ion LET for four different frequencies and five paths through the switch.

Figure 6 shows the BER for one path through the switch. It has the same overall behavior and, as expected, is approximately one fifth of the BER for the case of 5 paths through the switch.

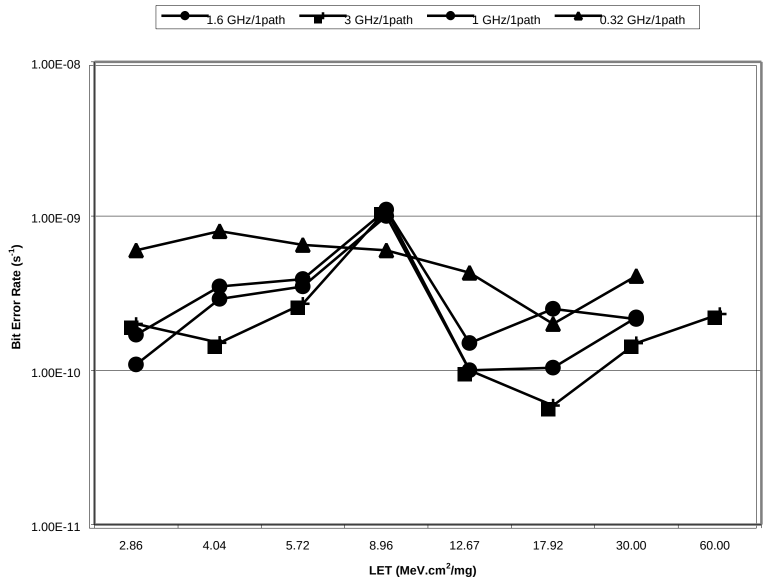

Figure 6. Single bit error rate as a function of ion LET for different data rates and for one pass through the switch.

Figure 7 shows the burst event rate as a function of effective LET for one path through the switch. The LET threshold for burst events is below 2.86 MeV.cm^2/mg. The dependence on LET seems to depend on data rate.

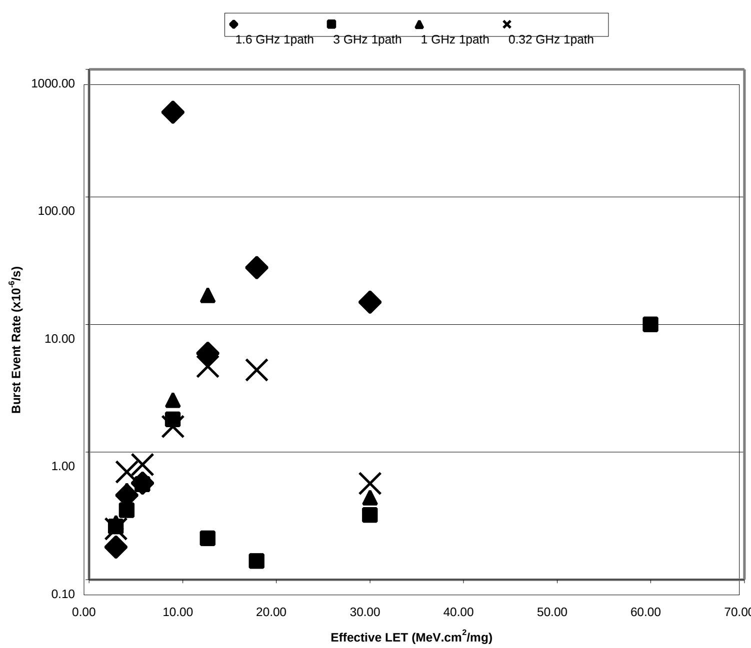

Figure 7. Burst event rate as a function of effective LET for 1 path through the switch and for different data rates.

Figure 8 shows the burst event rate as a function of ion LET for 5 paths through the switch. The LET threshold is also below 2.86 MeV.cm^2/mg. There is a general increase in the burst rate with ion LET. but the dependence on data rate is not clear.

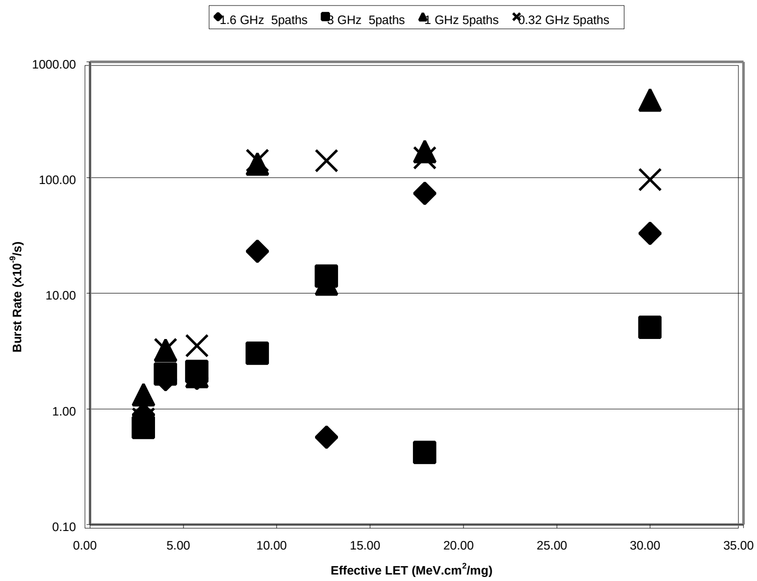

Figure 8. Burst event rate as a function of effective LET for five paths through the switch and for different data rates.

Figure 9 shows the average burst length versus ion LET for different data rates for five paths through the switch. Below a LET of 5.72 MeV.cm^2/mg the average burst length is less than 10 bits. Above, the average burst length increases rapidly with LET. There is no clear dependence on data rate, with the highest data rate having the shortest burst length.

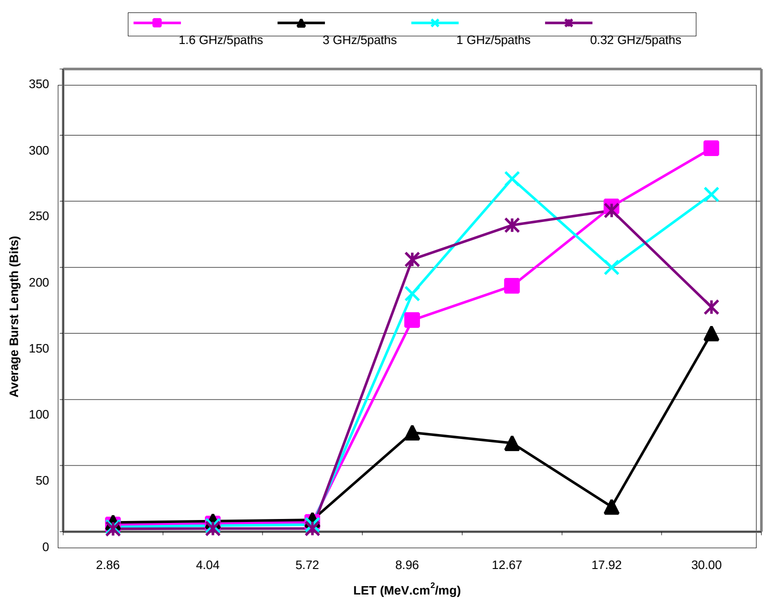

Figure 9. Average number of bits in a burst as a function of LET for 5 paths through the switch and for different bit error rates.

Figure 10 shows the average burst length for 1 path through the switch. The behavior is similar to that observed for five paths.

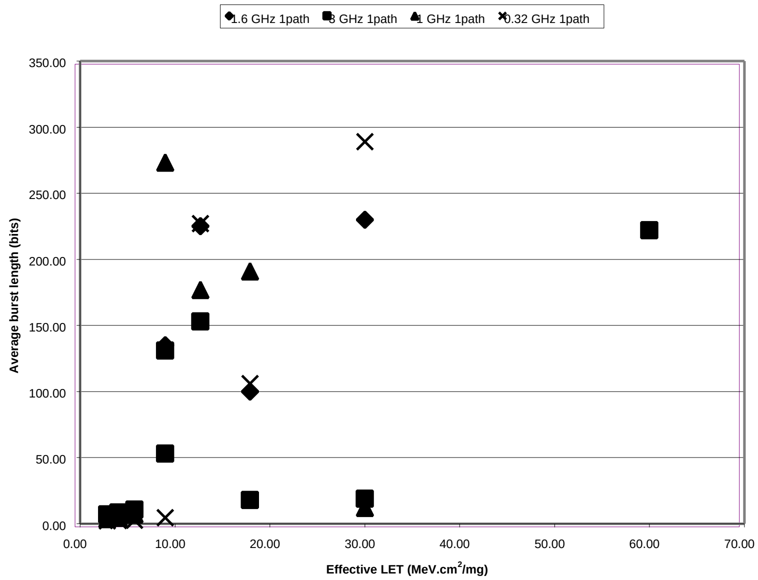

Figure 10. Average burst error length as a function of effective LET for different data rates and for one path through the switch.

Figure 11 shows the cross-section as a function of effective LET for loss-of-synchronization effects. The LET threshold for loss-of-synchronization is close to 8 $MeV.cm^2/mg$. There is a general increase in the cross-section with LET but there is no obvious dependence on data rate.

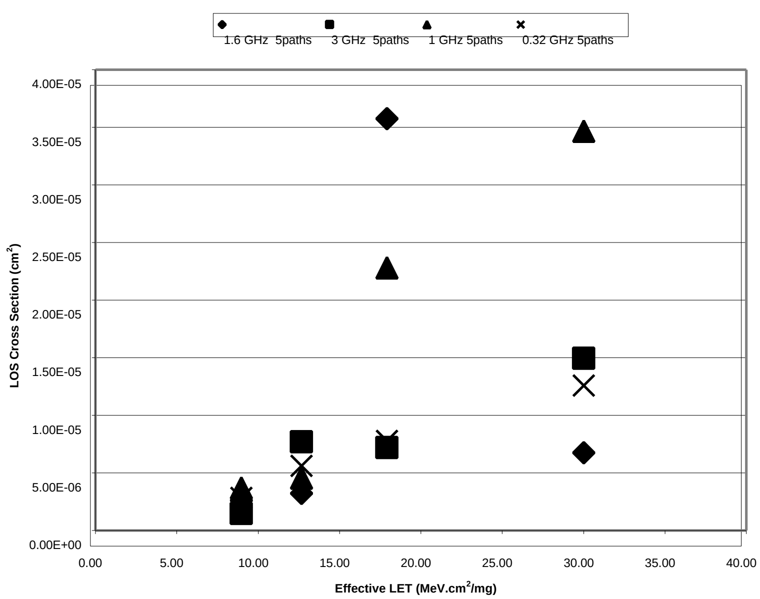

Figure 11. Loss of synchronization cross-section as a function of effective LET for four different data rates and five paths through the switch.

Figure 12 shows the LOS cross section as a function of ion LET for one path through the switch. The general trend is that the cross-section increases with LET but there appears to be no obvious dependence on data rate.

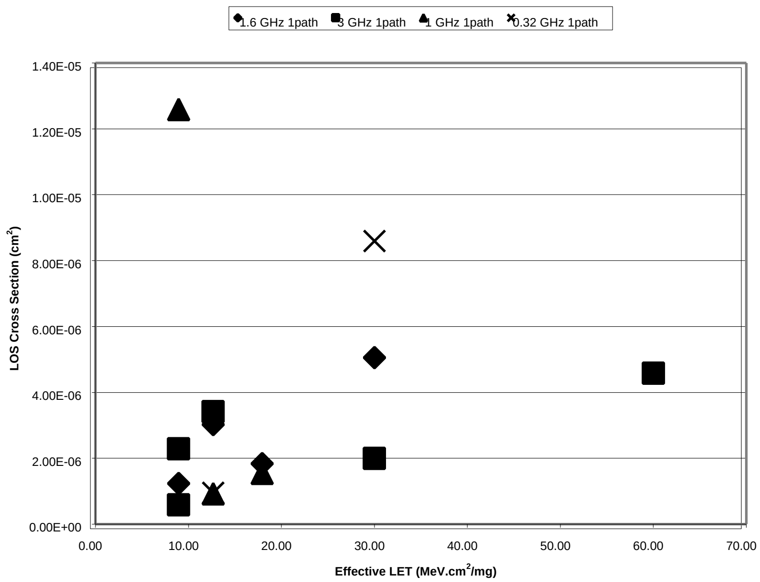

Figure 12. Loss of synchronization cross-section as a function of effective LET for four different data rates and for 1 path through the switch.

5. Conclusions

The AD8151 has been tested for SEEs using heavy ions. The part does not latch up but it does suffer from loss of synchronization. Both single bit errors and bursts of errors were observed. Bit error rates were found to depend on ion LET. Although the BERs showed a dependence on data rate, there was no obvious explanation.

Run No.	I_V_{EE} (mA)	# of paths	Ion	Tilt	LET	Effect. LET	Total fluence	Effect. fluence	Expos. Time	Data Rate (Gbps)	Total bits	Loss of Synch	Non-Burst Errors	Burst Errors	Total Errors	Burst Events	Total Events
1	161	5	Ne	0	2.86	2.86	5.34E+06	5.34E+06	128	3	3.84E+11		292	1888	2180	265	557
2	161	5	Ne	0	2.86	2.86	2.00E+06	2.00E+06	44	1.6	7.04E+10		35	366	401	71	106
3	161	5	Ne	0	2.86	2.86	2.00E+06	2.00E+06	44	1.6	7.04E+10		35	286	321	54	89
4	161	5	Ne	0	2.86	2.86	1.99E+06	1.99E+06	42	1	4.20E+10		24	188	212	56	80
5	161	5	Ne	0	2.86	2.86	1.99E+06	1.99E+06	41	1	4.10E+10		29	202	231	53	82
6	161	5	Ne	0	2.86	2.86	2.00E+06	2.00E+06	42	0.32	1.34E+10		35	21	56	10	45
7	161	5	Ne	0	2.86	2.86	2.01E+06	2.01E+06	42	0.32	1.34E+10		35	28	63	12	47
8	71	1	Ne	0	2.86	2.86	1.98E+06	1.98E+06	46	3	1.38E+11		29	221	250	33	62
9	71	1	Ne	0	2.86	2.86	2.02E+06	2.02E+06	42	3	1.26E+11		25	252	277	36	61
10	71	1	Ne	0	2.86	2.86	2.02E+06	2.02E+06	42	1.6	6.72E+10		6	87	93	18	24
11	71	1	Ne	0	2.86	2.86	2.02E+06	2.02E+06	40	1.6	6.40E+10		7	29	36	6	13
12	71	1	Ne	0	2.86	2.86	2.02E+06	2.02E+06	40	1	4.00E+10		8	46	54	11	19
13	71	1	Ne	0	2.86	2.86	1.99E+06	1.99E+06	38	1	3.80E+10		5	35	40	11	16
14	71	1	Ne	0	2.86	2.86	1.98E+06	1.98E+06	37	0.32	1.18E+10		5	12	17	5	10
15	71	1	Ne	0	2.86	2.86	1.99E+06	1.99E+06	40	0.32	1.28E+10		10	2	12	1	11
16	71	1	Ne	45	2.86	4.04	2.84E+06	2.01E+06	64	3	1.92E+11		29	512	541	62	91
17	71	1	Ne	45	2.86	4.04	2.83E+06	2.00E+06	84	3	2.52E+11		37	835	872	99	136
18	71	1	Ne	45	2.86	4.04	2.84E+06	2.01E+06	37	1.6	5.92E+10		21	119	140	21	42
19	71	1	Ne	45	2.86	4.04	2.81E+06	1.99E+06	38	1.6	6.08E+10		14	203	217	35	49
20	71	1	Ne	45	2.86	4.04	2.80E+06	1.98E+06	34	1	3.40E+10		9	66	75	14	23
21	71	1	Ne	45	2.86	4.04	2.85E+06	2.02E+06	36	1	3.60E+10		16	98	114	21	37
22	71	1	Ne	45	2.86	4.04	2.84E+06	2.01E+06	33	0.32	1.06E+10		7	21	28	9	16
23	71	1	Ne	45	2.86	4.04	2.83E+06	2.00E+06	34	0.32	1.09E+10		12	15	27	6	18
24	161	5	Ne	45	2.86	4.04	2.82E+06	1.99E+06	31	3	9.30E+10		210	1388	1598	190	400
25	161	5	Ne	45	2.86	4.04	2.83E+06	2.00E+06	29	3	8.70E+10		191	1450	1641	169	360
26	161	5	Ne	45	2.86	4.04	2.85E+06	2.02E+06	30	1.6	4.80E+10		65	483	548	84	149
27	161	5	Ne	45	2.86	4.04	2.80E+06	1.98E+06	29	1.6	4.64E+10		65	527	592	85	150
28	161	5	Ne	45	2.86	4.04	2.77E+06	1.96E+06	24	1	2.40E+10		34	425	459	93	127
29	161	5	Ne	45	2.86	4.04	2.81E+06	1.99E+06	24	1	2.40E+10		39	273	312	61	100
30	161	5	Ne	45	2.86	4.04	2.82E+06	1.99E+06	26	0.32	8.32E+09		42	70	112	29	71
31	161	5	Ne	45	2.86	4.04	2.87E+06	2.03E+06	27	0.32	8.64E+09		38	65	103	26	64
32	161	5	Ne	60	2.86	5.72	4.02E+06	2.01E+06	39	3	1.17E+11		346	2418	2764	269	615
33	161	5	Ne	60	2.86	5.72	4.02E+06	2.01E+06	43	3	1.29E+11		269	2187	2456	246	515
34	161	5	Ne	60	2.86	5.72	4.02E+06	2.01E+06	49	1.6	7.84E+10		116	1071	1187	149	265
35	161	5	Ne	60	2.86	5.72	3.96E+06	1.98E+06	51	1.6	8.16E+10		97	1032	1129	144	241
36	161	5	Ne	60	2.86	5.72	4.00E+06	2.00E+06	53	1	5.30E+10		76	618	694	115	191
37	161	5	Ne	60	2.86	5.72	3.97E+06	1.99E+06	60	1	6.00E+10		62	526	588	99	161
38	161	5	Ne	60	2.86	5.72	4.03E+06	2.02E+06	59	0.32	1.89E+10		46	165	211	65	111
39	161	5	Ne	60	2.86	5.72	3.97E+06	1.99E+06	53	0.32	1.70E+10		48	150	198	61	109
40	71	1	Ne	60	2.86	5.72	4.04E+06	2.02E+06	53	3	1.59E+11		41	1028	1069	96	137
41	71	1	Ne	60	2.86	5.72	4.04E+06	2.02E+06	48	3	1.44E+11		41	589	630	73	114
42	71	1	Ne	60	2.86	5.72	3.98E+06	1.99E+06	53	1.6	8.48E+10		33	550	583	65	98
43	71	1	Ne	60	2.86	5.72	3.96E+06	1.98E+06	53	1.6	8.48E+10		25	299	324	32	57
44	71	1	Ne	60	2.86	5.72	4.01E+06	2.01E+06	53	1	5.30E+10		19	206	225	28	47
45	71	1	Ne	60	2.86	5.72	3.97E+06	1.99E+06	53	1	5.30E+10		23	205	228	32	55
46	71	1	Ne	60	2.86	5.72	3.98E+06	1.99E+06	52	0.32	1.66E+10		7	30	37	11	18
47	71	1	Ne	60	2.86	5.72	3.97E+06	1.99E+06	50	0.32	1.60E+10		15	40	55	15	30
48	71	1	Ar	0	8.96	8.96	1.71E+06	1.71E+06	14	3	4.20E+10	1	28	4704	4732	67	95
49	71	1	Ar	0	8.96	8.96	0.00E+00	0.00E+00	0	3	0.00E+00		4	386	390	10	14
50	71	1	Ar	0	8.96	8.96	1.71E+06	1.71E+06	15	3	4.50E+10	1	49	4794	4843	93	142
51	71	1	Ar	0	8.96	8.96	5.26E+05	5.26E+05	5	1.6	8.00E+09	1	6	234743	234749	991	997
52	71	1	Ar	0	8.96	8.96	2.57E+05	2.57E+05	3	1.6	4.80E+09	1	3614	207647	211261	8243	11857
53	71	1	Ar	0	8.96	8.96	2.99E+05	2.99E+05	3	1.6	4.80E+09	1	7	316618	316625	1501	1508
54	71	1	Ar	0	8.96	8.96	2.00E+06	2.00E+06	70	1.6	1.12E+11	0	40	1145	1185	68	108
55	71	1	Ar	0	8.96	8.96	1.64E+05	1.64E+05	6	1.6	9.60E+09	1	6	258603	258609	1381	1387
56	71	1	Ar	0	8.96	8.96	3.17E+05	3.17E+05	12	3	3.60E+10	1	11	3876	3887	22	33
57	71	1	Ar	0	8.96	8.96	5.58E+05	5.58E+05	20	3	6.00E+10	1	47	12911	12958	149	196
58	71	1	Ar	0	8.96	8.96	2.00E+06	2.00E+06	74	1	7.40E+10	0	61	19684	19745	190	251

Run No.	I_V_{EE} (mA)	# of paths	Ion	Tilt	LET	Effect. LET	Total fluence	Effect. fluence	Expos. Time	Freq. (GHz)	Total bits	Loss of Synch	Non-Burst Errors	Burst Errors	Total Errors	Burst Events	Total Events
59	71	1	Ar	0	8.96	8.96	7.94E+04	7.94E+04	3	1	3.00E+09	1	4	679554	679558	2486	2490
60	71	1	Ar	0	8.96	8.96	2.00E+06	2.00E+06	75	0.32	2.40E+10	0	20	182	202	39	59
61	71	1	Ar	0	8.96	8.96	1.99E+06	1.99E+06	74	0.32	2.37E+10	0	8	171	179	37	45
62	161	5	Ar	0	8.96	8.96	8.88E+05	8.88E+05	31	3	9.30E+10	1	105	2536	2641	102	207
63	161	5	Ar	0	8.96	8.96	4.82E+05	4.82E+05	17	3	5.10E+10	1	103	32581	32707	252	355
64	161	5	Ar	0	8.96	8.96	3.01E+05	3.01E+05	11	1.6	1.76E+10	1	30	4620	4650	42	72
65	161	5	Ar	0	8.96	8.96	4.64E+05	4.64E+05	17	1.6	2.72E+10	1	29	241568	241597	1162	1191
66	161	5	Ar	0	8.96	8.96	4.02E+05	4.02E+05	15	1	1.50E+10	1	27	255884	255911	1501	1528
67	161	5	Ar	0	8.96	8.96	1.39E+05	1.39E+05	5	1	5.00E+09	1	16	157621	157637	822	838
68	161	5	Ar	0	8.96	8.96	5.23E+05	5.23E+05	21	0.32	6.72E+09	1	15	191029	191044	685	700
69	161	5	Ar	0	8.96	8.96	1.80E+05	1.80E+05	7	0.32	2.24E+09	1	35	54580	54615	402	437
70	161	5	Ar	45	8.96	12.67	8.01E+03	5.66E+03	1	3	3.00E+09	1	43	9612	9655	86	129
71	161	5	Ar	45	8.96	12.67	3.59E+05	2.54E+05	66	3	1.98E+11	1	52	1626	1678	68	120
72	161	5	Ar	45	8.96	12.67	6.79E+05	4.80E+05	137	1.6	2.19E+11	1	54	33393	34199	173	227
73	161	5	Ar	45	8.96	12.67	1.99E+05	1.41E+05	39	1.6	6.24E+10	1	11	3966	3977	22	33
74	161	5	Ar	45	8.96	12.67	3.23E+05	2.28E+05	54	1	5.40E+10	1	25	164982	165007	760	785
75	161	5	Ar	45	8.96	12.67	2.97E+05	2.10E+05	51	1	5.10E+10	1	27	163984	164011	518	545
76	161	5	Ar	45	8.96	12.67	2.47E+05	1.75E+05	43	0.32	1.38E+10	1	19	395915	395934	1911	1930
77	161	5	Ar	45	8.96	12.67	2.56E+05	1.81E+05	45	0.32	1.44E+10	1	7	528282	528289	2050	2057
78	71	1	Ar	45	8.96	12.67	1.49E+05	1.05E+05	23	3	6.90E+10	1	10	3785	3795	16	26
79	71	1	Ar	45	8.96	12.67	6.80E+05	4.81E+05	121	3	3.63E+11	1	22	4702	4724	68	90
80	71	1	Ar	45	8.96	12.67	3.96E+05	2.80E+05	74	1.6	1.18E+11	1	15	146490	146505	720	735
81	71	1	Ar	45	8.96	12.67	5.40E+05	3.82E+05	99	1.6	1.58E+11	1	13	234727	234740	925	938
82	71	1	Ar	45	8.96	12.67	1.26E+05	8.91E+04	19	1	1.90E+10	1	3	152954	152957	630	633
83	71	1	Ar	45	8.96	12.67	1.41E+06	9.97E+05	209	1	2.09E+11	0	31	495	526	39	70
84	71	1	Ar	45	8.96	12.67	2.03E+04	1.44E+04	3	0.32	9.60E+08	1	14	1316421	1E+06	6103	6117
85	71	1	Ar	45	8.96	12.67	1.47E+06	1.04E+06	207	0.32	6.62E+10	0	15	74051	74066	311	326
86	71	1	Ar	60	8.96	17.92	2.00E+06	1.00E+06	282	3	8.46E+11	0	50	2073	2123	127	177
87	71	1	Ar	60	8.96	17.92	1.00E+06	5.00E+05	132	3	3.96E+11	0	18	1060	1078	53	71
88	71	1	Ar	60	8.96	17.92	1.24E+06	6.20E+05	180	1.6	2.88E+11	1	30	230233	230263	1468	1498
89	71	1	Ar	60	8.96	17.92	9.37E+05	4.69E+05	129	1.6	2.06E+11	1	3602	456408	460010	10609	14211
90	71	1	Ar	60	8.96	17.92	1.81E+06	9.05E+05	236	1	2.36E+11	1	46	272683	272729	1303	1349
91	71	1	Ar	60	8.96	17.92	7.80E+05	3.90E+05	91	1	9.10E+10	1	28	847937	850812	4901	4929
92	71	1	Ar	60	8.96	17.92	2.00E+06	1.00E+06	244	0.32	7.81E+10	0	13	169	182	33	46
93	71	1	Ar	60	8.96	17.92	1.00E+06	5.00E+05	152	0.32	4.86E+10	0	12	84536	84548	406	418
94	161	5	Ar	60	8.96	17.92	3.82E+05	1.91E+05	67	3	2.01E+11	1	65	1853	1918	78	143
95	161	5	Ar	60	8.96	17.92	1.75E+05	8.75E+04	26	3	7.80E+10	1	33	534	567	36	69
96	161	5	Ar	60	8.96	17.92	5.52E+04	2.76E+04	9	1.6	1.44E+10	1	4	223011	223015	888	892
97	161	5	Ar	60	8.96	17.92	5.67E+04	2.84E+04	9	1.6	1.44E+10	1	7	297086	297093	1225	1232
98	161	5	Ar	60	8.96	17.92	1.47E+05	7.35E+04	24	1	2.40E+10	1	13	280604	280617	1293	1306
99	161	5	Ar	60	8.96	17.92	2.84E+04	1.42E+04	5	1	5.00E+09	1	1	262439	262440	1420	1421
100	161	5	Ar	60	8.96	17.92	6.72E+04	3.36E+04	11	0.32	3.52E+09	1	6	183160	183166	866	872
101	161	5	Ar	60	8.96	17.92	4.48E+05	2.24E+05	79	0.32	2.53E+10	1	29	348284	348313	1264	1293
102	161	5	Kr	0	30	30.00	4.47E+04	4.47E+04	0	3	0.00E+00		51	363883	363934	1610	1661
103	161	5	Kr	0	30	30.00	7.57E+04	7.57E+04	13	3	3.90E+10	1	38	5101	5139	60	98
104	161	5	Kr	0	30	30.00	5.82E+04	5.82E+04	10	3	3.00E+10	1	35	29271	29306	258	293
105	161	5	Kr	0	30	30.00	4.15E+04	4.15E+04	7	1.6	1.12E+10	1	7	183313	183320	616	623
106	161	5	Kr	0	30	30.00	2.55E+05	2.55E+05	45	1.6	7.20E+10	1	59	249163	249222	891	950
107	161	5	Kr	0	30	30.00	3.96E+04	3.96E+04	7	1	7.00E+09	1	4	7106	7110	30	34
108	161	5	Kr	0	30	30.00	1.81E+04	1.81E+04	3	1	3.00E+09	1	5	760664	760669	2811	2816
109	161	5	Kr	0	30	30.00	7.14E+04	7.14E+04	14	0.32	4.48E+09	1	34	6186	6220	101	135
110	161	5	Kr	0	30	30.00	8.75E+04	8.75E+04	20	0.32	6.40E+09	1	17	304282	304299	1084	1101
111	71	1	Kr	0	30	30.00	5.03E+05	5.03E+05	122	3	3.66E+11	0	55	2143	2198	133	188
112	71	1	Kr	0	30	30.00	5.00E+05	5.00E+05	133	3	3.99E+11	1	33	2387	2420	106	139
113	71	1	Kr	0	30	30.00	9.46E+04	9.46E+04	28	1.6	4.48E+10	1	8	228970	228978	1130	1138
114	71	1	Kr	0	30	30.00	3.01E+05	3.01E+05	108	1.6	1.73E+11	1	44	230607	230651	875	919
115	71	1	Kr	0	30	30.00	5.59E+05	5.59E+05	166	1	1.66E+11	0	28	633	661	62	90
116	71	1	Kr	0	30	30.00	4.00E+05	4.00E+05	115	1	1.15E+11	0	30	794	824	58	88
117	71	1	Kr	0	30	30.00	5.68E+05	5.68E+03	2	0.32	6.40E+08	1	2	457771	457773	2240	2242
118	71	1	Kr	0	30	30.00	2.27E+05	2.27E+05	66	0.32	2.11E+10	1	7	4495	4502	12	19
119	71	1	Kr	60	30	60.00	1.22E+05	6.10E+04	33	3	9.90E+10	1	23	270601	270624	980	1003
120	71	1	Kr	60	30	60.00	5.85E+04	2.93E+04	17	3	5.10E+10	1	11	229575	229586	998	1009
121	71	1	Kr	60	30	60.00	1.13E+06	5.65E+05	284	3	8.52E+11	1	8	4296	4304	27	35